Journal of Structural Geology, Vol. 6, No. 3, pp. 303 to 319, 1984
Printed in Great Britain

0191-8141/84 $03.00 + 0.00

Shear bands, crenulations and differentiated layering in ice–mica models

C. J. L. WILSON

School of Earth Sciences, University of Melbourne, Parkville, Victoria 3052, Australia

(*Received* 3 *March* 1983; *accepted in revised form* 19 *October* 1983)

Abstract—Thin sheets of composite ice–mica have been deformed in order to simulate the development of cleavages in quartz–mica rocks. A strong initial mica preferred orientation was variably oriented to the shortening direction. Deformation parallel to the foliation results in a crenulation type cleavage developing from shear bands initiated after a component of pure shear. Deformation oblique to the foliation produces a differentiated cleavage and involves a large component of shear strain subparallel to the original anisotropy. The strain is accommodated by intra- and intercrystalline processes that produce extensive grain elongation and rearrangement of the ductile matrix, thereby forming ice vs mica rich regions. On the other hand, there is no drastic morphological change when a sample is shortened perpendicular to an original foliation: that is, where the micas lie in the plane of no shear strain. Instead, the mica fabric is strengthened and the grains in the ductile matrix are flattened.

Two models are presented for the initiation, propagation and evolution of the observed crenulation versus differentiated cleavage types. These depend on mica stacking and orientation relative to the transverse properties of the sample and also on the direction of anisotropy to the XY plane of the bulk strain ellipsoid. The models invoke shear on planes of high shear strain and rotation of the shear bands and rigid mica grains into a direction approximately parallel to the bulk extension direction.

INTRODUCTION

THE EXPERIMENTS described here were designed to simulate deformation in a foliated quartz–mica rock. The model material chosen was ice with finely dispersed mica. The ice–mica particle composites were prepared in the manner described by Wilson (1983). The study was undertaken using a time-lapse photographic system to try and obtain some insight into the deformation processes operating on a bulk scale during the mechanical rotation of mica in a polycrystalline matrix. The ice matrix undergoes plastic deformation with intracrystalline slip on the basal plane with no preferential slip direction in that plane (Kamb 1961) at temperatures in the range of −8°C and combined intracrystalline slip and solid state diffusional processes at higher temperatures such as −1°C (Wilson & Russell-Head 1982). Unlike quartz-rich metamorphic rocks, there is no pore fluid contributing to the total deformation observed in these experiments.

It has been demonstrated (e.g. Cobbold *et al.* 1971, Means & Williams 1972, Gray 1979, Means *et al.* (in press) that strong planar mineral anisotropy exerts an important control on folding and foliation development. This is particularly so for features such as crenulation cleavages which fold earlier mineral fabrics. A number of experimental attempts (see review by Means 1977) have been undertaken to model such cleavages by compressing strongly oriented analogue materials. These studies, often on bulk samples and constrained by rigid boundary conditions, have yielded ideal fold forms (e.g. Bayly 1969, Latham 1979) but little information on the sequential development of the fabric, except for the study of Means *et al.* (in press). In this paper it is proposed to describe the mechanical rotation of strongly oriented platy elements during pure-shear plane strain deformations where the samples are unconstrained perpendicular to the bulk extension direction (X). This produces incremental and non-uniform shortenings together with shear and the formation of crenulation-type cleavage zones. Unlike other experimental studies (e.g. Means & Williams 1972, Means *et al.* in press, Wilson 1983), the platy elements are not completely free to undergo passive rotation in their ductile matrix. It is suggested in this paper that this is a major factor contributing to the formation of crenulation cleavage and of domainal cleavages.

EXPERIMENTAL METHODS

The experiments were performed in the apparatus illustrated in Fig.1. The specimen (approximately 40 × 20 × 0.7 mm) was deformed between two glass plates by driving a 0.7 mm thick platen into the thin sample (0.7 mm) at a constant rate (Table 1). The surfaces of the sample were lubricated with a film of silicon oil and during the deformation the sample was contained in a silicon oil bath. The deforming specimen was viewed in transmitted light by means of a video camera and the dynamic events were recorded either on 35 mm film or by using a time lapse camera on 16 mm cine film. The deformation stage and all cameras were mounted on a supporting frame that was placed within an insulated container in a freezer chest set typically at −20°C. The air temperature within the insulated container and hence the experiments (Table 1) were then maintained using a balance between a platinum resistance thermometer bridge and a set of heaters attached to the air circulating fans (Fig. 1).

The experiments were carried out at a strain rate of either 8.7 or $2.9 \times 10^{-7}\ s^{-1}$ (Table 1). The cyclic

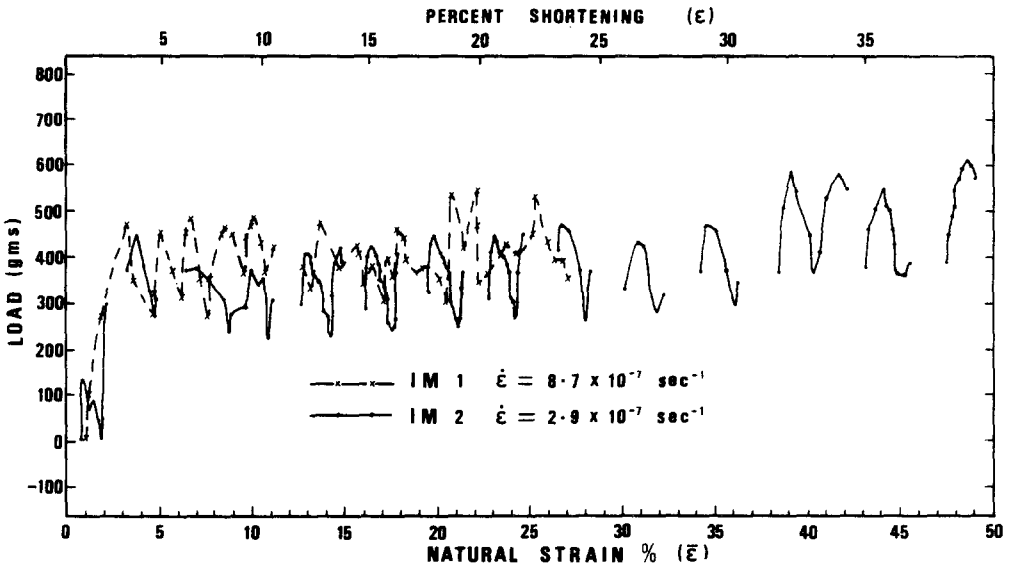

Fig. 2. Load vs strain curves illustrating the behaviour of the ice–mica aggregate during experiments IM1 and IM2. The breaks in the curves represent periods where no readings were taken.

mechanical behaviour (Fig. 2) was first thought to correspond to dynamic changes in the sample but these could not be detected. Subsequent modification of the apparatus has shown that the cyclic behaviour was a function of motor-gearbox effects. If an enveloping surface is drawn to the peak of maximum load it can be seen that slightly higher loads (Table 1) were required to deform the sample at the faster strain rate. The stresses during a deformation varied from 0.28 to 0.35 MPa.

All the ice–mica samples used were 0.7 mm thick slabs cut from a block of ice–mica particle composites used in other experiments by Wilson (1983). The matrix ice is composed of polycrystalline randomly oriented grains with diameters of approximately 0.3 mm. The sample was selected so that the cleavage planes of the mica platelets were near vertical to the constraining glass plates and parallel to the direction of plane strain, Y. The initial mica preferred-orientation in a sample was oriented either parallel, 60° or normal to the bulk shortening direction, Z (Table 1). The orientation of (001) mica traces with respect to the bulk shortening axis (Z), plotted as histograms, were taken from photomicrographs.

EXPERIMENTAL RESULTS

Mica fabric parallel to shortening direction

Three stages of the sequence observed in model IM1 are illustrated in Figs. 3 (a–c). The deformation is initially accommodated by the ice matrix with little rotation of the micas. The specimen uniformly increases in width parallel to X and any air-bubbles, contained within the grain boundaries are expelled in the first 5% shortening. The air bubbles migrate to, and are forced out into, the silicon oil that occupies the space between the specimen and the constraining glass plates. The deformation then becomes non-homogeneous with the first obvious area of mechanical rotation of micas occurring in a zone adjacent to the moving platen (zone 1, Fig. 3a). This noticeable rotation of the micas begins to occur after approximately 10% shortening. At 20% shortening (Fig. 3b) there is marked evidence for mica realignment in zone 1, a weaker realignment in zone 2 and very little change in zone 3. By 20% shortening the strong initial mica preferred-orientation (Fig. 3d) has decreased (Fig. 3e) and with further deformation the overall mica fabric becomes markedly bimodal (Fig. 3f).

Table 1. Summary of *in situ* ice–mica experiments. All experiments were undertaken at −1°C except for IM5 which was −8°C

Experiment number	Initial mica orientation with respect to shortening axis, Z(degrees)	Experiment duration (days)	Shortening (%)	Strain rate $\times 10^{-7} s^{-1}$
IM1	0	5	37.5	8.7
IM2	0	13	39.1	2.9
IM3	0	14	40	2.9
IM4	0	6	30	8.7
IM5	60	5	27	8.7
IM6	60	5	24	8.7
IM7	90 (and 0)	4	28	8.7

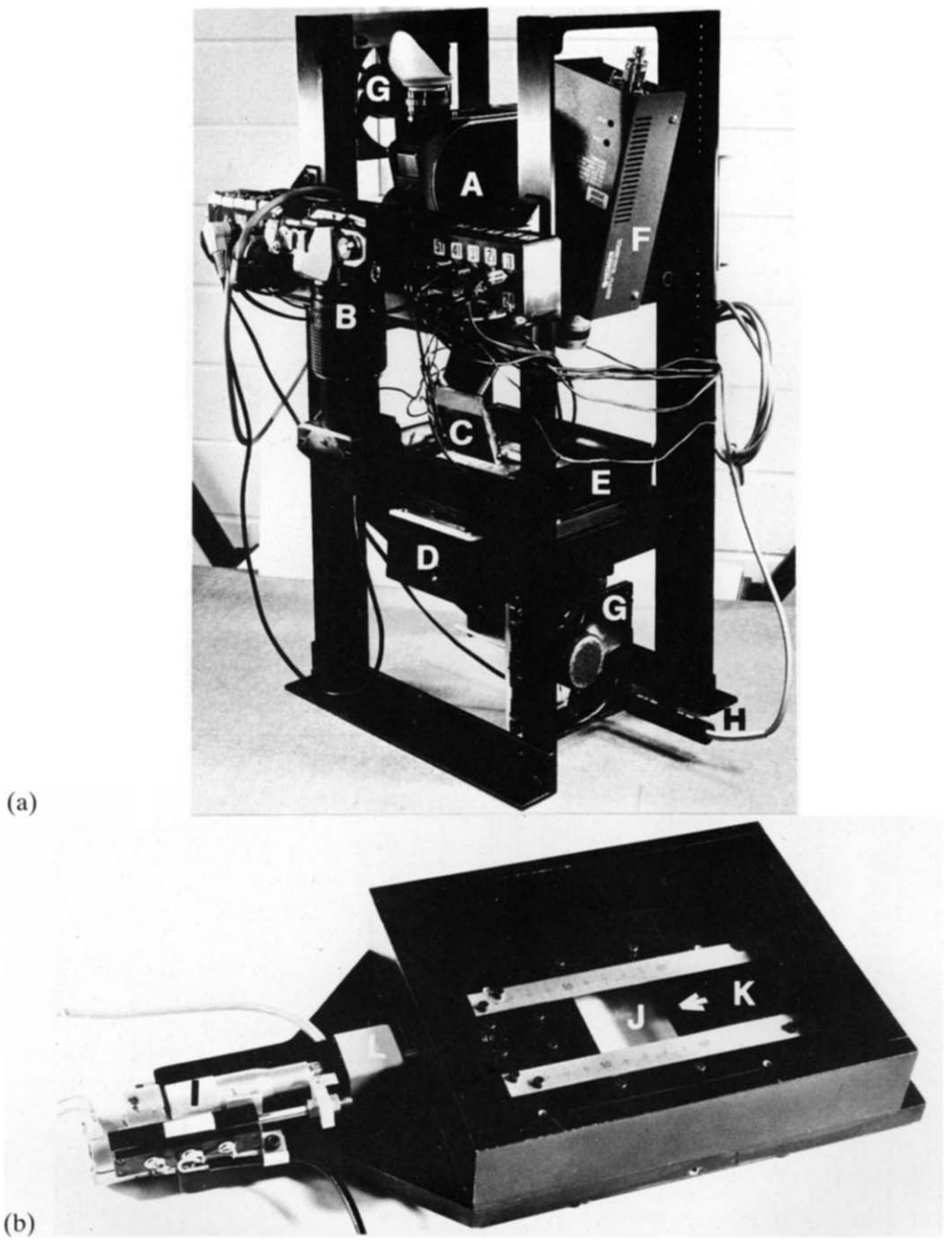

Fig. 1. Plane strain deformation apparatus. (a) shows the arrangement of the cameras to the deformation apparatus. A. Bolex 16 mm movie camera that sits directly above the specimen; B, 35 mm camera with mirror angled at 45° and obtains image from mirror C which is moved into position above the specimen by a solonoid motor when a photograph is required. Mirror C normally sits to one side during cinematography. D is light source under deformation stage E. F is video camera used to survey the specimen during an experiment. G fans used for air circulation and H is the temperature probe. (b) Details of deformation stage showing: I, motor drive and gear box; J, position of specimen; K, deforming platen with principal direction of motion indicated which corresponds to the bulk shortening direction Z; L, load cell.

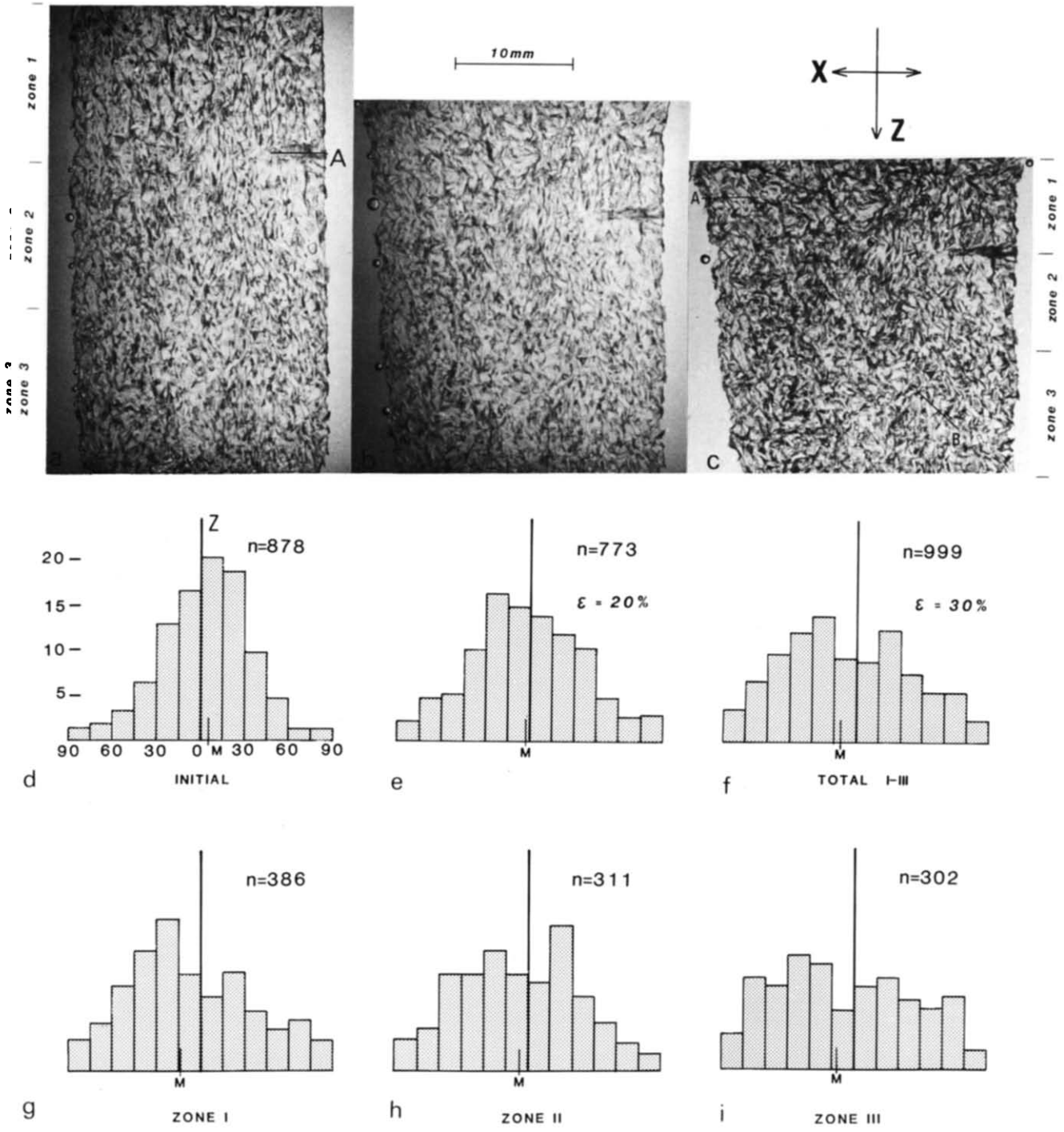

Fig. 3. Three stages in the shortening of IM1, the base of the sample is fixed and the deforming platen moves in the direction Z parallel to the predominant initial mica orientation. (a) is the initial sample, (b) after 20% and (c) after 30% shortening. (d–f) are the (001) mica orientations with respect to the shortening axis. (g–i) are frequency histograms of mica orientations representing the angle between the trace of (001) and the shortening axis Z in zones I–III at stage (c). M, mean.

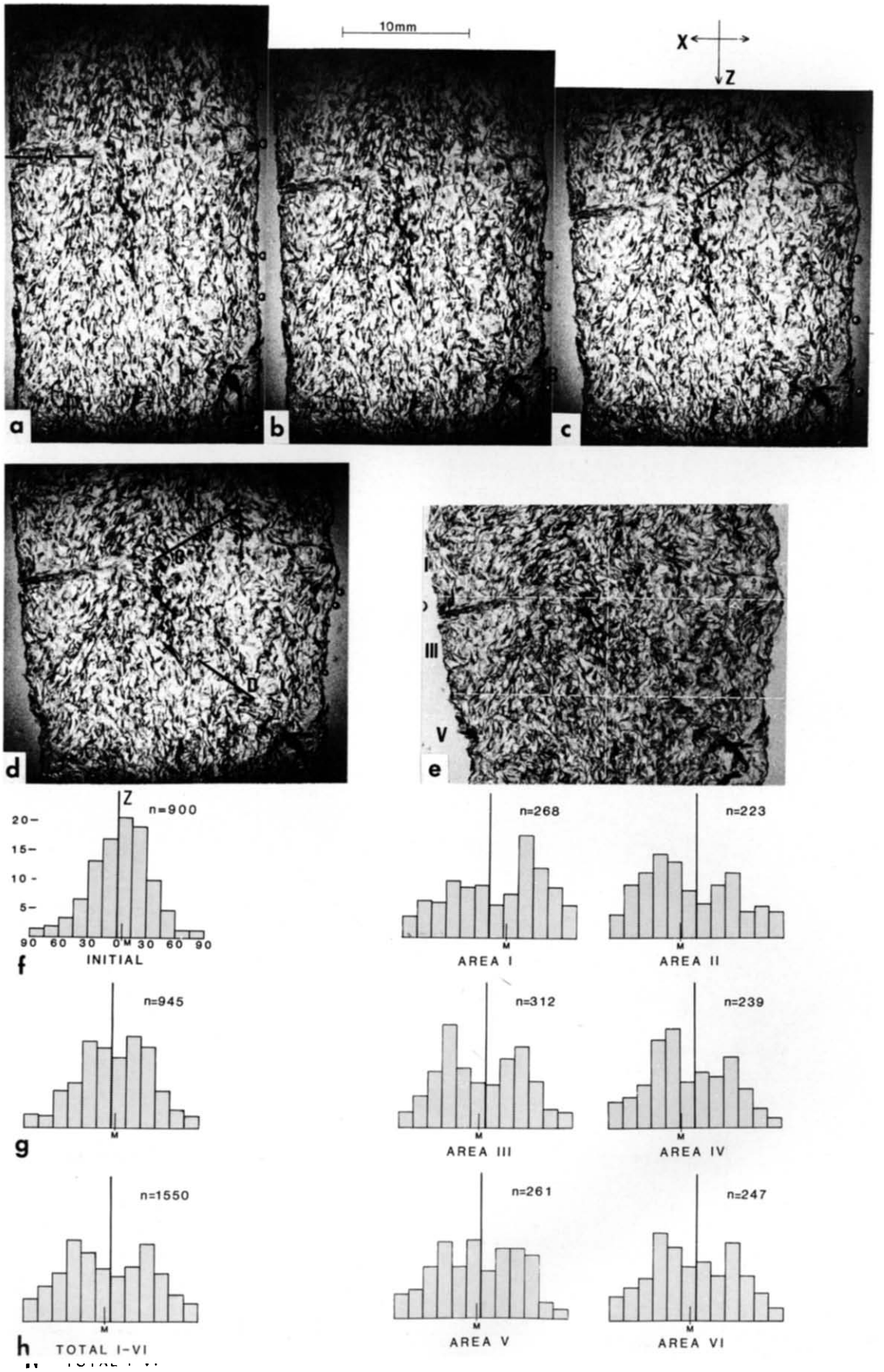

Fig. 4. Deformation of IM2 and mica (001) distributions measured with respect to the shortening axis *Z*. (a) is initial sample, (b) 13%, (c) 20%, (d) 29% and (3) 39% shortening. The mica distributions (f–h) correspond to stages (a), (c) and (3). The mica distributions from individual areas I–VI correspond to the final stages of deformation (e). M, Mean.

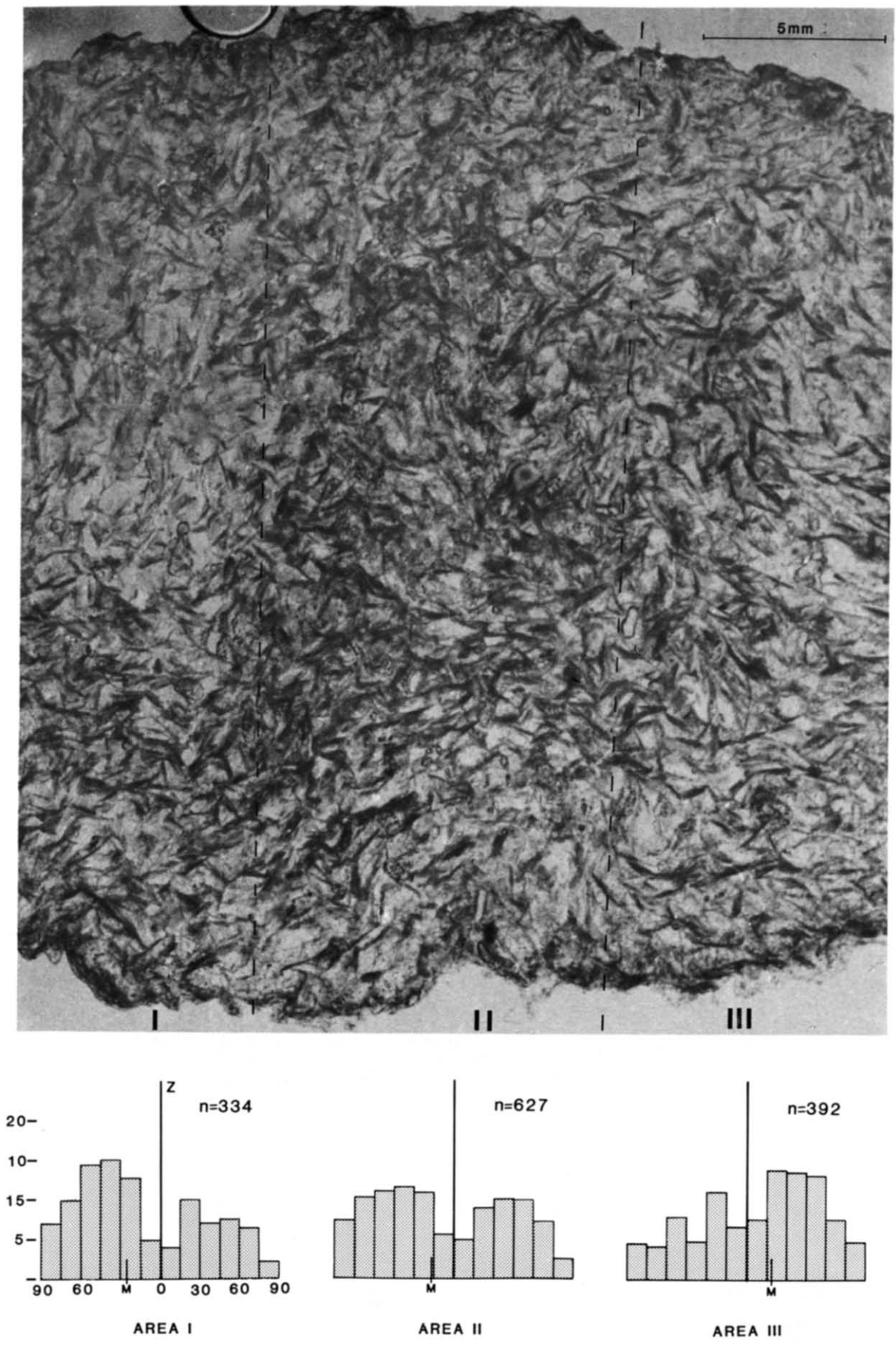

Fig. 6. Sample IM3 after 40% shortening and mica (001) distributions in zones I–III with respect to Z.

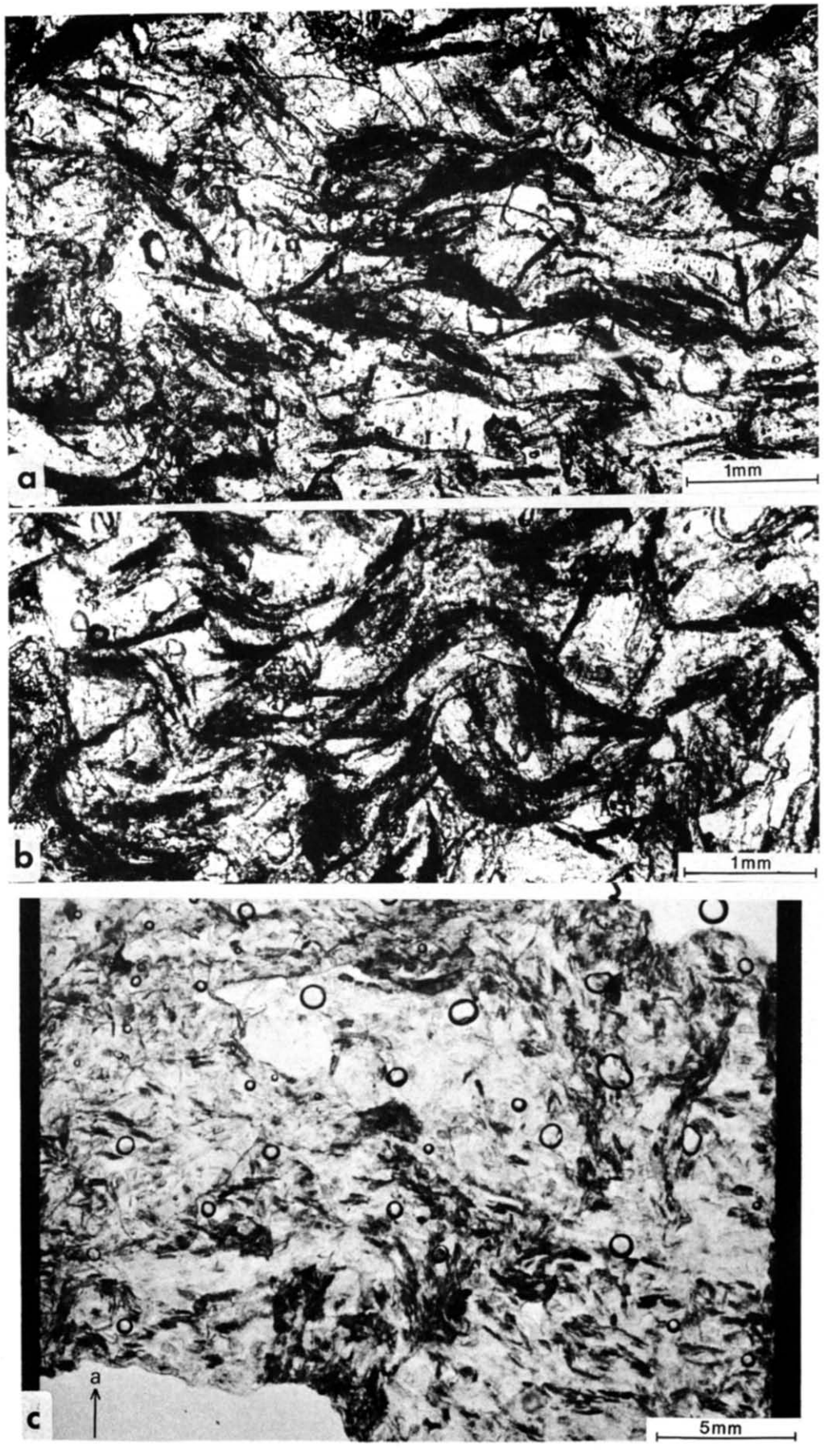
a
1mm
b
1mm
c
a
5mm

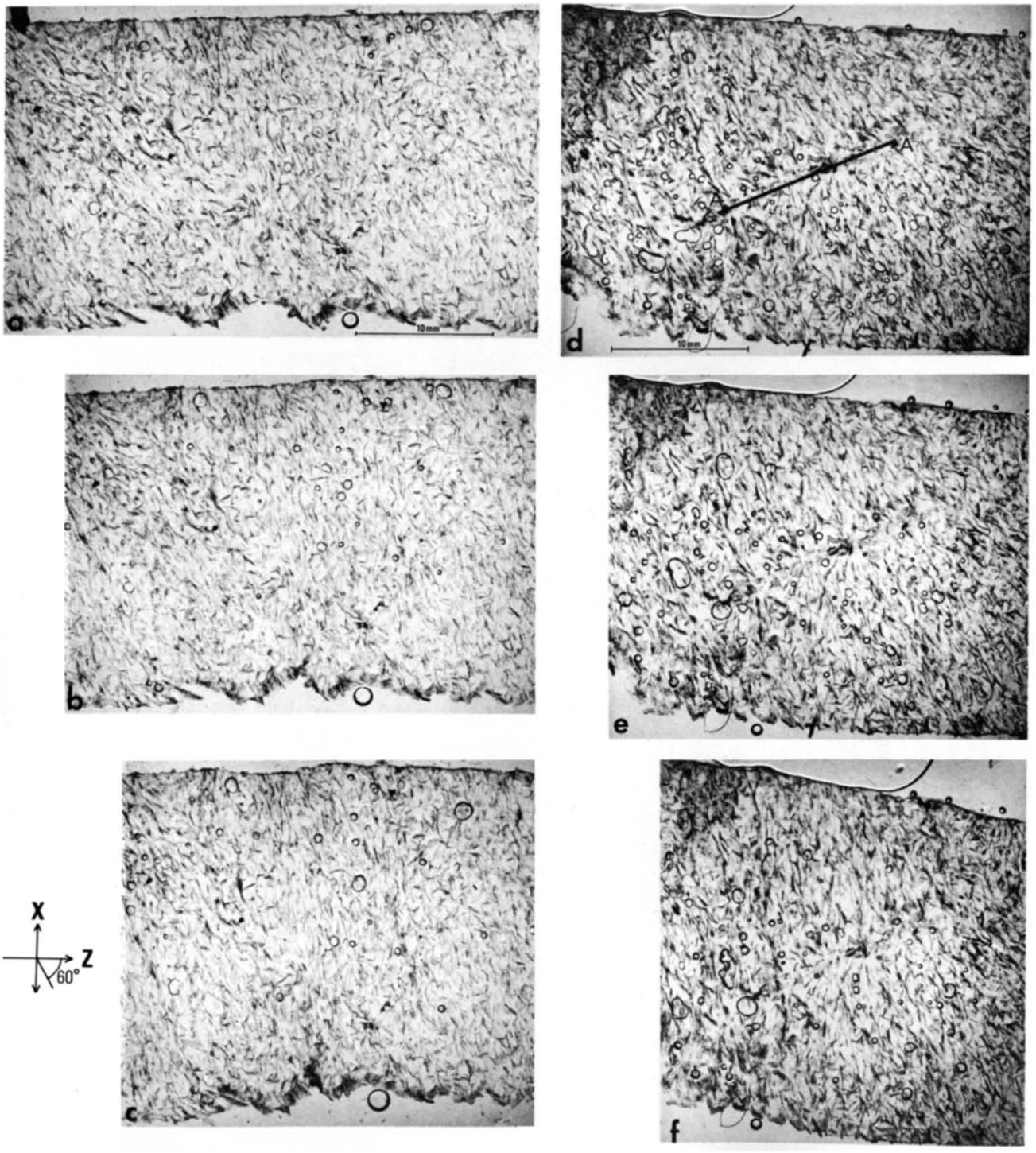

Fig. 8. Deformation sequence in IM5 (a–c) and IM6 (d–f) illustrating the initial sample where the initial mica preferred orientation was 60° from the shortening direction Z (a, d), the 12% (b, e) and the 24% (c, f) shortening stages. Photographed in plane polarized light.

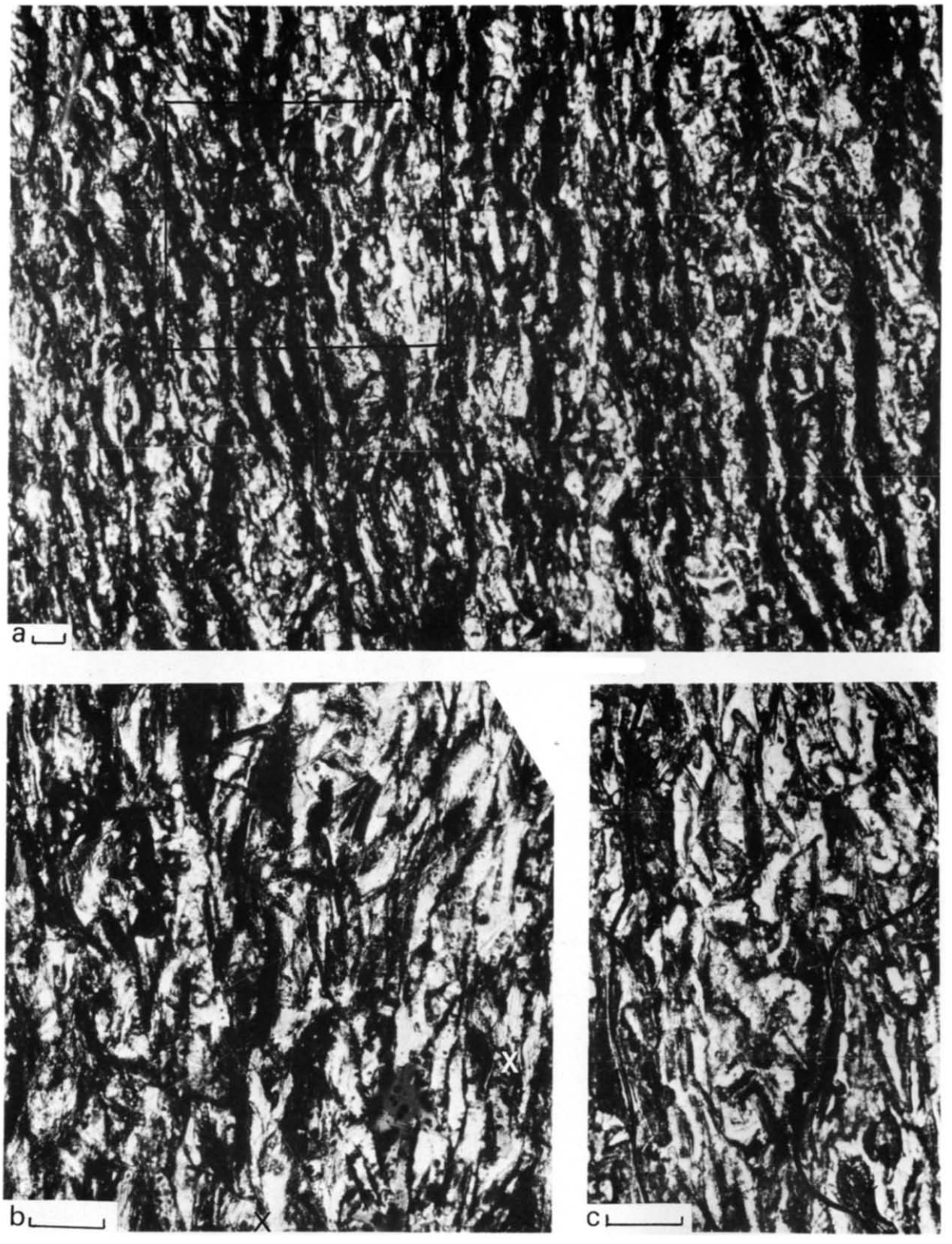
a
b
X
X
c

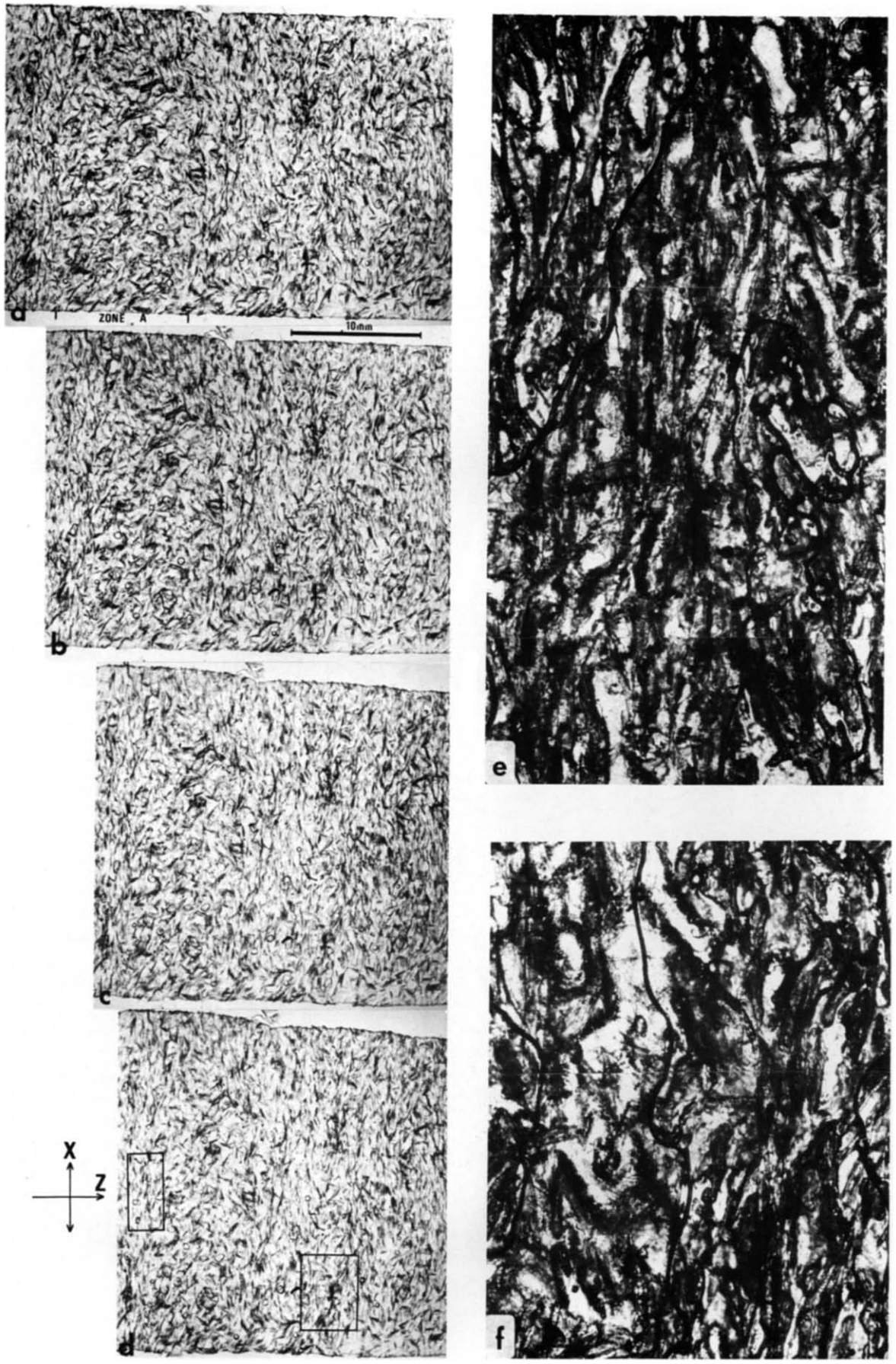

Fig. 10. Deformation sequence in IM7 (a–d) at 2, 12, 23 and 28% shortening photographed in plane polarized light. Micrographs (e–f) taken with partially crossed nicols showing the distribution of ice (white) between micas in the areas outlined in (d).

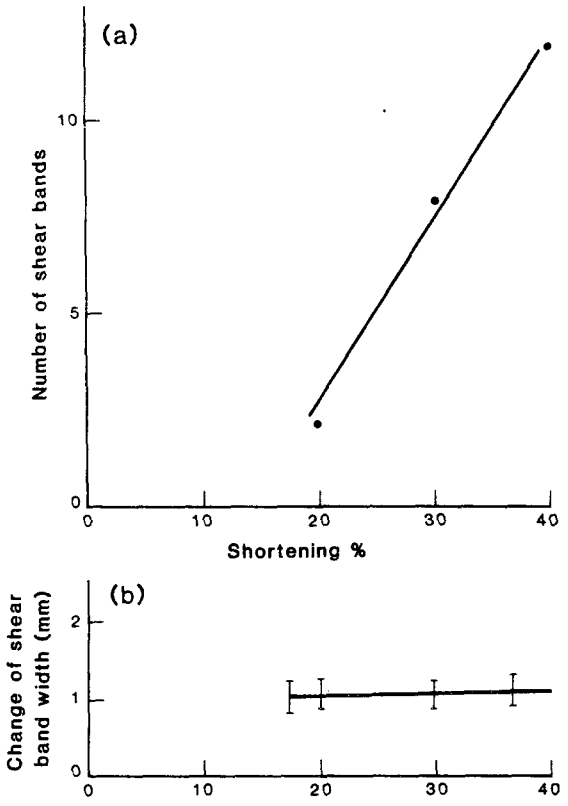

Fig. 5. (a) Generalized curve derived from experiment IM2 demonstrating that distinct shear bands are only recognized after 10% shortening. At greater shortenings the number of shear bands may be higher than portrayed here as the initiation of shear bands is difficult to recognize using the photographic system employed to record these experimental results. (b) Range in width of a series of shear bands in IM2 with progressive shortening.

The redistribution of the micas between 20 and 30% shortening is non-uniform across the sample. The micas are markedly asymmetric in the more deformed zone (Fig. 3g) with a transition to a uniform distribution in zone 3 (Fig. 3i). Associated with the change in the mica fabric is the formation of areas of more marked mica rotation (Fig. 3c, subparallel to A in zone 1) that appear to have been initiated at 50° to Z (B in Fig. 3c).

Figure 4 shows a deformation of a similar sample at a slower strain rate but with greater shortening. Again there is very little change in the mica fabric until after 10% shortening. The initial strain is confined to the ice matrix, as seen by comparing the ice-rich area A (Fig. 4a) with the same area after 13% shortening (Fig. 4b). The first marked changes are undulations created on the surface of the specimen (area B, Fig. 4b) as a direct result of deformation in the ice matrix. Only after 15% shortening has a noticeable rotation of the micas occurred adjacent to the moving platen (area C, Fig. 4c); reorientation of the micas is insignificant at the other end of the sample. The mica rotation is asymmetric and occurs in a zone oriented at approximately 55° to the shortening axis. An opposite sense of rotation is then developed in a conjugate zone (area D, Fig. 4d) that becomes more accentuated with further deformation (Fig. 4e). The zones where this asymmetry in the fabric is noted have the appearance of 'shear bands'; that is, narrow bands where the deformation within each band is predominantly one of shear parallel to the interface of the band and the adjacent material, as commonly described in anisotropic metals. It should be noted that during progressive deformation the shear bands increase in number (Fig. 5a), and are of limited and unchanged width (Fig. 5b). It is only their length and orientation that changes with increased sample shortening.

The inclination of the shear bands at C and D to the shortening axis is ±50° (±5°). These angles change with increasing strain (e.g. the band at C increases to 70° by the end of the experiment) and bands increase in number (Fig. 4e) and become more pronounced at larger strains. As a consequence the overall mica fabric becomes wavier (Fig. 4e). The change from a strong initial mica orientation distribution (Fig. 4f) to a weak bimodal fabric begins with the first appearance of the shear bands (Fig. 4g) but is markedly obvious in the final fabric (Fig. 4h). However, the mica fabric in individual areas may be markedly asymmetric (Fig. 4e, areas I–VI). For instance, areas I and II have the highest asymmetry, being regions containing the earliest formed shear bands. It is in these regions that the shear bands have spread laterally; in so doing the micas undergo a sense of rotation compatible with the sense of shear in the shear band.

Although experiments IM1 (Fig. 3) and IM2 (Fig. 4) have similar starting materials there are obvious differences. In IM1 the linear area of ice (A in Fig. 3a) undergoes no rotation whereas the comparable area in IM2 is significantly rotated with a shear strain of 0.17. Also in IM2 there is a noticeable development of shear bands (parallel to D in Fig. 4d) and a non-homogeneous extension in the X direction. This suggests that the initiation of the shear bands and the formation of a pseudo-crenulation cleavage is dependent on the extent of non-uniformity in the extensional strain.

A bimodal mica distribution was also observed in experiment IM3 (Fig. 6) with opposite senses of mica asymmetry adjacent to the reaction and action platens (Figs. 6b & d) and a symmetric mica rotation in the centre of the sample. Deformation was non-homogeneous across the sample and occurred as a series of progressive zones. Again in this sample the mica redistribution was produced by localized shear bands progressively rotated during deformation into an orientation subperpendicular to Z and subparallel to X. This accounts for the symmetric distribution in the centre of the sample. In a general way the deformation features appear similar to the sinusoidal buckles observed by Cobbold *et al.* (1971, Fig. 8). However, no features directly comparable to kink bands were observed in any of the experiments IM1–3.

During progressive deformation the reoriented mica platelets initially retain their planar form being rigid objects in a ductile ice matrix. The degree of mica reorientation may reflect the shortening strain but only when there is a homogeneous deformation of the supporting matrix (Wilson 1983). However, in areas of shear band development bent micas become noticeable

(Fig. 7a) with marked curvature in the better defined shear bands (Fig. 7b). This curvature appears to be a result of the non-uniform strain across a shear band and is not due to platelet interaction as has been discussed by Oertel & Phakey (1972) and Tullis (1976). Additional evidence that mica curvature is associated with the superimposed shear bands is seen in an experimental failure (Fig. 7c). (Because of camera malfunctions there was no record of the progressive deformation). In this sample only the mica platelets adjacent to the shear zones show marked curvature.

Mica fabric oblique to shortening direction

In experiments IM5 and IM6 where the initial mica fabric is inclined (Table 1) there is progressive rotation of individual mica platelets (Fig. 8) into an orientation subparallel to X. There is little evidence for the development of conjugate shear bands and there are only a few bent micas; these were micas initially subparallel to the shortening axis. One notable feature of these experiments is the accentuation of the pre-existing foliation.

In IM5 there is marked anastomosing of the foliation which is defined by a strong orientation of mica aggregates and individual micas (Fig. 9b) alternating with elongate lenses of highly deformed ice possessing deformation lamellae and undulose extinction. In some areas of IM5 the foliation could be referred to as domainal with alternating ice vs mica rich zones (Fig. 9a). In IM6 the foliation is in part domainal but is typically anastomosing around elongate aggregates of coarse interlocking ice grains. Another difference between IM5 and IM6 is that the ice contains an abundance of deformation lamellae in IM5 (Fig. 9b) and a paucity in IM6 (Fig. 9c). The ice microstructure in IM6 suggests extensive grain growth and is comparable to that recognized in other deformed polycrystalline aggregates (Wilson & Russell-Head 1982).

Experiment IM5 involved essentially a pure-shear deformation whereas IM6 has a component of simple shear parallel to X initiated after 10% shortening (Fig. 8e), as the sample slipped at the interface with the deforming platens. The small component of shear and flattening occur simultaneously with progressive shortening (Fig. 8f), with little change in orientation of pre-existing planar features such as the ice marker A–A (Figs. 8d–f). There was no diagnostic feature to suggest the existence of a shearing or a non-coaxial strain component in either the mica or ice microstructures.

Mica fabric normal and parallel to shortening direction

Experiment IM7 had two initial mica orientation components; the majority of the micas were oriented perpendicular to the shortening direction, between which was a zone of highly misoriented micas (Zone A, Fig. 10a). During progressive shortening there was little change in the spatial relationship between micas. The strongly aligned micas rotated into orientations perpendicular to Z with individual ice grains becoming elongate between the mica platelets. Micas in Zone A were rotated, many were bent and individual separation distances became smaller with individual ice grains in the matrix tending to aggregate into larger ice rich areas between the deformed micas.

DISCUSSION

Interpretation of experimental observations

In the mica-parallel deformation (IM1–3) there was initially a component of pure shear, but with increasing strain there was the development of localized shear zones or two-dimensional shear bands. These could be thought of as areas that undergo localized strain softening; however, the formation of these shear bands could not be correlated with any overall reduction in stress. The shear bands appear to be initiated as two conjugate sets $\pm 55°$ to the shortening direction, but were not initiated simultaneously. They appear to develop after the ductile deformation of the ice, occurring during the first 10% shortening. The first-formed shear bands become rotated whereas the second set lies approximately parallel to the complementary shear plane. Morphologically and genetically, these shear bands resemble shear bands produced during the deformation of metals (Dillamore *et al.* 1979, Anand & Spitzig 1980). As in the metals they begin to occur after the breakdown of homogeneous flow (i.e. the pure-shear component of deformation), and are thought to be a consequence of the strong anisotropy exerted by the mica fabric.

The ice–mica composites are examples of an anisotropic material deformed by means of a ductile matrix with the subsequent mechanical rotation of the enclosed particles. This type of deformation is in contrast to other experimental studies using anisotropic materials where slip and rotation occurs on layers with negligible internal deformation with the production of kink bands (Paterson & Weiss 1966, Cobbold *et al.* 1971, Reches & Johnson 1976, Weiss 1980). In the latter type of experiment overall deformation is accommodated by increasing the width of a constantly oriented kink band. In contrast (e.g. Fig. 5b), the shear strain across the shear bands in IM1–3 may increase but the width appears to be independent of the progressive shortening. There is also a rotation of the shear band together with concurrent layer parallel shortening in the material outside the shear band. These observations are similar to those of Means *et al.* (1983) but not comparable to the kink experiments.

It should be noted that the experiments were conducted on finite-dimensional specimens whereas previous studies of particle rotation in a ductile matrix have used composite blocks. Further, a state of uniform in-plane uniaxial compression, prior to the initiation of the shear bands and the crenulation type patterns, was not attained in these experiments. This factor may control the initiation of the shear bands and explain the progressive and non-uniform stages of deformation and varying degree of mica reorientation across any sample.

There is also a mechanical problem with mica platelets being unable to rotate in the third dimension. This may partly account for the curvature observed in some micas. However, it should be noted that where mica bending occurs it is always in an area of shear band development and hence areas of higher strain.

In experiments IM1–3 the shear bands are initiated after 15% shortening and in IM6 a small amount of shear parallel to the foliation is initiated after 10% shortening. This is in marked contrast to the foliated rock models described by Wilson (1983) where shear and shortening strains were occurring together from the onset of the deformation. In the foliated rock model experiments (Wilson 1983), even in areas of high rotational strain, there was little evidence for bent mica, which is certainly not true for the present experiments. This difference in mica behaviour may be attributed to two factors. (1) A three-dimensional effect, where micas in the foliated rock models were unconstrained and free to undergo mechanical rotation at a sufficiently fast rate, so that there is no mechanical locking of the materials on a grain scale and hence an increase in the yield strength. (2) The strong mica orientation coupled with the confined three-dimensional thickness forced the micas or bundles of micas to act as barriers and stopped the flow of the ice matrix. The latter depends on the length, the density and spatial distribution of the micas. Therefore, a long mica or continuous mica aggregates in a soft matrix will not rotate easily; instead, as further strain increments are added the sample can only yield by shearing and therefore the initiation of the shear bands is essentially governed by the micas rather than the matrix.

The shortening superimposed on the earlier foliation in IM7 is akin to simple flattening with no significant locking of the grain structure nor redistribution of ice. It is only in regions containing misoriented micas that a different mechanical behaviour occurs; that is mica bending is observed with a local redistribution of ice into larger aggregates. Redistribution of the ice matrix occurs on a larger scale in IM5 and IM6 with the generation of anastomosing foliations and the mica versus ice-rich domains that subparallel the original mica preferred-orientation. This is in marked contrast to the starting material which contained uniformly distributed ice and mica. These observations imply that the strong local mica concentrations and orientations are due to the local strain or the collapse of the mica into regions depleted of ice. A major problem is the identification of the driving mechanisms for this differentiation.

In rocks, differentiation has been variously ascribed to a difference in stress, in pressure, or in chemical potential between differently oriented limb and hinge regions of a crenulated foliation (Cosgrove 1976, Fletcher 1977, Gray 1979, Vidale 1974, Weber 1981, Williams 1972). The majority of geological arguments invoke a pore fluid permeating the composite (e.g. Gray 1979, Williams 1972). However, in these experiments, particularly in IM5, there is certainly no evidence for any fluid phase or the operation of bulk diffusive processes. In fact the diffusivity of the ice is too low to account for such transport (Glen 1975, Weertman 1968). It appears that differentiation may be wholly or dominantly a result of heterogeneous flow; that is, the ice has been preferentially 'squeezed' out between the mica platelets. The main means of differentiation must be intracrystalline slip which is also responsible for the very marked ice grain elongation and may be accompanied by some intercrystalline deformation. Slip in the mica is difficult to establish; however, some micas in IM5–6 do have a fuzzy appearance and are slightly bent which may be due to a combination of elastic strain and failure by shearing on the cleavage. Evidence for intergranular deformation with sliding on mica grain boundaries could not be observed in these experiments.

The differentiation also appears to be controlled by the orientation of the foliation relative to the axes of applied stress. Mechanical rearrangement of the more ductile ice matrix only occurs where there are high shear stresses subparallel to the stiffer micas. The fact that differentiation effects are better developed in specimens deformed at lower temperatures than at higher temperatures is further evidence that differentiation is affected by purely mechanical processes and not purely diffusion-operated processes. The operation of similar mechanical processes to produce differentiation has also been described by Means & Williams (1972) in dry samples of foliated salt–mica mixtures.

The origin of shear bands and crenulations

A consequence of these experiments is that the initiation and morphology of secondary cleavages may be very dependent on the role of the mica in controlling the ductile flow of the matrix between the dispersed phase. The dispersed micas will have a yield strength much less sensitive to plastic deformation than a single piece of mica of the same shape and orientation as the ice–mica sample. The obvious reason for this is that the geometry ensures that the deformation will either be parallel and/or across the (001) mica anisotropy resulting in kink bands (Etheridge *et al.* 1973). Therefore, the strength of the ice–mica composite is governed by failure of the micas. In these experiments and in quartz–mica rocks containing discontinuous micas it is necessary to look at the question of how the micas successfully stiffen the material.

Figure 11 illustrates the origin of the observed shear bands and the development of the crenulation type cleavages in IM1–3. The homogeneous strain in the matrix changes the horizontal and longitudinal separation of the mica particles. As the longitudinal separation decreases the dispersed mica phase becomes more interlocked and with greater overlap. A consequence of this is that the flow of the ductile ice between the rigid micas is probably restricted in the horizontal direction by bridging micas. This initially increases the strength of the material by the development of rectilinear cells of ice constrained by mica platelets. Within the first 10% of shortening the ice matrix will develop a definite *c*-axis

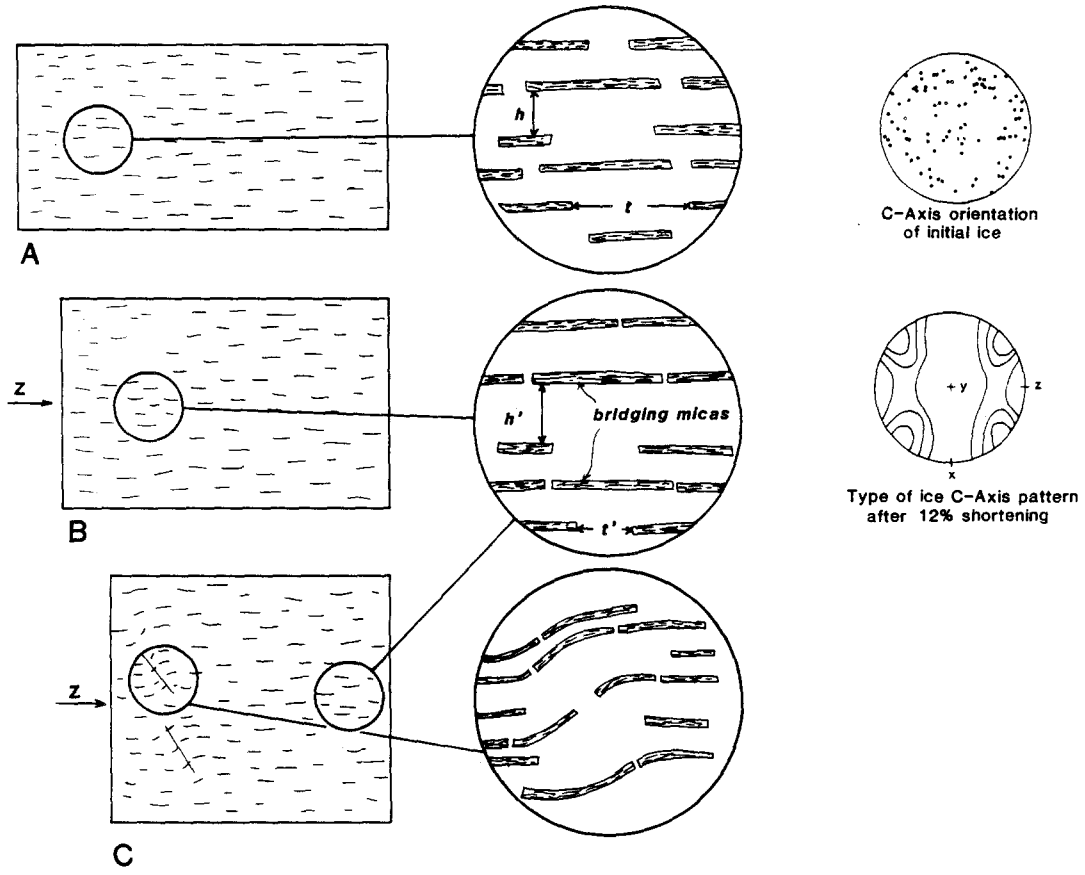

Fig. 11. Schematic illustrations of the superimposition of longitudinal shortening on mica particles dispersed in the ice matrix and the development of the shear bands. (a) The initial ice–mica sample with width x and length z. The micas are arranged with the lateral separation h and the longitudinal separation t. The ice matrix would have random c-axis orientations prior to deformation. (b) After 12% shortening the dimensions x' and h' have increased with a decrease in z' and t'. This results in the development of a rectangular cellular structure. The ice c-axis preferred orientation pattern would be a double maxima lying in a small circle girdle centred about Z. (c) After 20% shortening there is a rotation of the micas within shear bands in the region adjacent to the moving platen. At the other end of the sample the mica distribution is still similar to that observed at stage (b).

preferred orientation symmetrically related to the shortening direction (Wilson 1983, Wilson & Russell-Head 1982). This will also enhance the anisotropy of the material. The strengthening or stiffening generates an instability in the sample in a direction at a high angle to the longitudinal shortening. With the exceeding of the elastic limit bending occurs in the micas and the shear bands are propagated with the flow of the ice matrix in this direction. The ice grains in the matrix then yield by shearing and this may be governed by the Hall–Petch stress (Hirth & Lothe 1968) necessary for the transmission of yield from grain to grain and partly by the mica spacing.

It should be noted that the strengthening described here is different from the *foliation-strengthening* process described by Means (1981), who was referring to individual elements in a foliation moving towards a steady state preferred orientation and not a mechanical locking of the grain structure. Instead, the strengthening is a combination of both the ice fabric and the dispersed second phase micas. As pointed out by Ashby (1969), one of the reasons for this increased resistance to deformation is that the yield strength of the matrix would increase as a function of particle strength known as the Orowan Stress. In fact the hard particles would increase the critical shear stress at its interface with the ductile matrix. The value of the shear stress would fall off rapidly with distance from the particle. It would be in the matrix, away from the hard particle, that the greatest intracrystalline slip would occur. This area would therefore be the site that generates the instability that produces the shear band structures at stage C of the model (Fig. 11).

At stage C (Fig. 11), the model is superficially similar to the salt–mica experiments of Means & Williams (1972, fig. 10). However, there are significant differences; Means & Williams (1972) deformed their samples perpendicular to the foliation and the 'fault-like' structures they generated may be a function of the constraining jacket. The ice–mica experiment (IM7) of comparable orientation never developed such shears. The type of instability that may generate the shear bands in the ice–mica experiments would arise from differences in layer-parallel and layer-normal stresses at the contacts between the micas versus the matrix grains. The presence of this type of instability in a foliated material has caused the onset of a *foliation-weakening* process (Means 1981). This results in the local disordering and reduction of the strong dimensional preferred-orientation of the micas through a shearing process similar to

that described by Means (1981, fig. 4). However, the major contributor to this is the role of intracrystalline processes in the ductile matrix.

It may be argued that during the stiffening of the ice–mica composite (Fig. 11) the degree of isotropy of the in-plane mechanical properties of the unidirectional mica aggregates may be controlled by the ratio of mica width w, to the thickness t, by the aspect ratio w/t. However, in all these experiments this ratio is rather high and it is believed that virtually isotropic properties are achieved. Instead it is the effects of mica aspect ratios, mica stacking patterns and orientation on the transverse properties of the sample that control the mechanical and microstructural development.

Model for differentiation

It has been suggested that the differentiation observed in IM5 and 6 are due to mechanical processes. The model adopted here for such a process is illustrated in Fig. 12 and relies on the fact that there is little rotation of the platy elements in the third dimension. Two features that appear to be significant in the formation of the domainal structures are:

(1) shear subparallel to the pre-existing foliation and

(2) the early foliation is progressively rotated into the XY plane of the bulk strain ellipsoid.

The onset of deformation (Fig. 12b) was marked by shortening in the ice matrix followed by elongation of the ice subparallel to the foliation. This elongation would be accompanied by a change in the shape of the ice grains as they accommodate the strain between the mica. Progressively increasing heterogeneous strain and shear subparallel to the dominant mica distribution enhances internal distortion and rigid body rotation, leading to elongate ice grains (Fig. 12c). As well as being strongly elongate there is also a uniform sense of shear as seen by the preferred orientation of deformation lamellae (Fig. 9b) and c-axes (Fig. 12c). As the matrix grains become more elongate the rigid micas sitting on grain boundaries move closer together and eventually aggregate as the ice moves into distinct zones (Fig. 12c). At the scale of observation used to record data in these experiments no evidence for grain boundary sliding as a mechanism could be established. There would be further rotation of the incremental and the developing foliation as the sample continues to undergo shortening (Fig. 12c).

Therefore, during a deformation the original foliation is rotated with a contribution of layer-parallel elongation and layer-parallel shear. This is comparable to the changes that occur to a layer situated on a fold limb (Bayly & Cobbold 1979) and to the sliding that may occur in asymmetric cleavage zones (see Knipe 1979, fig. 2e). The model also contains features suggested by Granath (1980) for natural rocks and the experiments described by Means *et al.* (in press). Considering the ice matrix only, such a model is also reconcilable with Etchecopar's (1977) geometrical models for two-dimensional deformation. However, the model is quite at

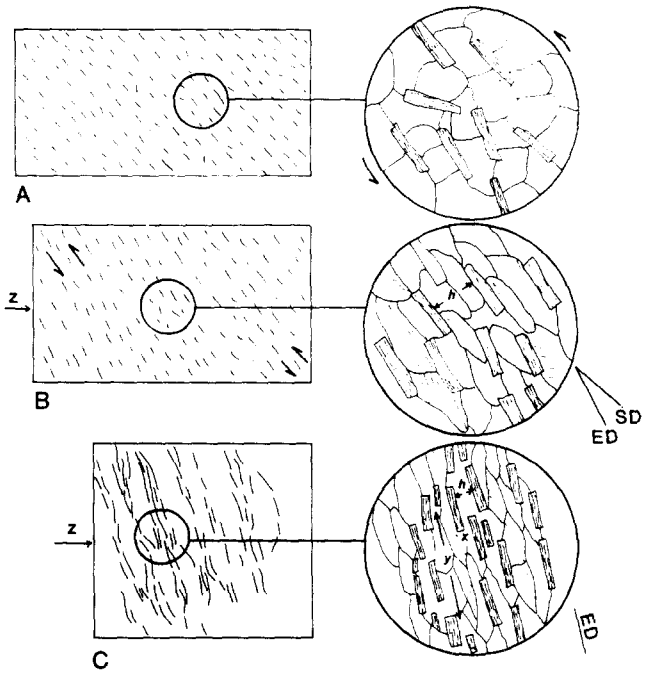

Fig. 12. Schematic diagram illustrating the development of differentiated layering by shearing subparallel to a pre-existing micaceous layering. (a) The initial ice–mica sample and accompanying grain structure with a uniform c-axis distribution in the ice. (b) After the initial increment of deformation (approximately 7% shortening) the ice grains are elongate with intracrystalline slip occurring on (0001), which appears as deformation lamellae. This will develop a new c-axis preferred orientation pattern as described by Wilson (1983). The ice grain shapes are constrained by the mica. Superimposed on this deformation is a component of shear strain subparallel to the strongly oriented micas with shear direction SD. (c) Further shear results in the development of a strong elongation direction (ED) in the ice with a reduction of the lateral separation h between the mica platelets and the development of attenuated mica rich regions. In places such as x there may be intercrystalline slip on ice–mica boundaries resulting in greater separation y between the elongate ice aggregate and juxtaposition of individual micas. Rotation of the elongate ice and mica foliation occurs with further shortening.

variance to the model suggested by Borradaile (1981) who wants grain boundary slip early in the development of a cleavage and intracrystalline processes occurring late. The reason for the difference may be the presence of pore fluids as suggested by Borradaile (1981). Another major difference between the models presented here and Borradaile's model is that the latter does not consider relative ductilities nor the distribution of the component phases that make up a rock.

The importance of a mechanical component during the formation of a differentiated layering was first advocated by Schmidt (1932) and questioned on a number of grounds by Shelley (1974). One of the arguments used by Shelley was that because quartz and mica are both relatively ductile they should not segregate and form a layering. However, contrary to Shelley's unsupported arguments there are obvious differences in the mechanical behaviour between quartz and mica (Wilson 1980). This therefore means that some of the processes suggested by Schmidt (1932) and observed in these analogue experiments could play an important role in cleavage formation in natural rocks. This is one of several deformation mechanisms that could be expected

in low-grade regional metamorphic rocks and its contribution to the formation of differentiated layering appears to have been overlooked in recent times, as there has been a popularity in the geological literature for some form of solution-assisted transport. One of the reasons why mechanical differentiation may have been overlooked, except in zones of high shear strain such as mylonites, is that the highly strained grains would be energetically the most favoured for dissolution. Therefore in the absence of evidence for pervasive intracrystalline slip, the grain structure would not directly reflect the true origin of the microstructure.

CONCLUSIONS

The *in situ* experiments described above indicate that in the absence of a fluid phase, mechanical processes and particularly the role of shearing can influence the morphological development of cleavage. By deforming a pre-existing foliation defined by oriented micas it has been found that cleavage morphologies depend on the following factors:

(1) a combination of the ductility contrast of mica versus the ductile matrix and the inability of the micas to rotate in the third dimension,

(2) orientation of the earlier foliation to the direction of maximum shortening,

(3) the amount of rotation individual mica platelets are capable of undergoing during realignment, itself dependent on initial spatial distribution and orientation,

(4) the extent of grain elongation accomplished by intracrystalline slip and/or intercrystalline slip processes in the ductile matrix, and

(5) whether intracrystalline slip is accompanied by grain growth processes which would govern the degree of differentiation.

In all experiments there has been progressive and non-uniform reorientation of the micas across the samples. The shear bands and crenulation-type cleavages produced in the layer-parallel deformations were generated after the sample undergoes shortening by intracrystalline deformation with a locking of the grain structure. The shear bands are probably initiated parallel to a plane of high shear strain. Once a shear band and a zone of rotated micas has been initiated, in a zone of high shear strain, it is then progressively rotated into an orientation subparallel to the XY plane of the bulk strain ellipsoid. Hence, after shortening strains of >35% there is evidence for shear strain along the foliation as well as for the approximate parallelism of the final orientation of the foliation to the XY plane of the bulk strain axes.

High shear strains subparallel to a pre-existing foliation may produce mechanical differentiation. The differentiation is well displayed where intracrystalline processes dominate (IM5) but weaker where grain growth accompanies the intracrystalline slip (IM6). Applying these observations to regional geological environments suggests that at lower temperatures where intracrystalline slip is an important process there is a greater likelihood for differentiation to occur. However, at higher grades where extensive recovery and grain growth relieve the strain, differentiation may not be as marked. On the other hand, where an early foliation remains perpendicular to the direction of maximum shortening (as in IM7) no strong differentiation would be expected as it is a plane of no shear strain and the grains would simply undergo flattening.

Acknowledgements—This work was financially supported under the Australian Research Grants Scheme. The Glaciology section of the Australian Antarctic Division provided the coldroom used for examination and preparation of the ice samples. David Russell-Head is thanked for his able redesign and building of the deformation apparatus and control units which has enabled the undertaking of these and the many other experiments that have led to the results and interpretations published in this paper. J. Mitchell is thanked for his technical help and W. D. Means, S. H. Treagus and S. H. White for their comments on the manuscript.

REFERENCES

Anand, L. & Spitzig, W. A. 1980. Initiation of localized shear bands in plane strain. *J. Mech. Phys. Solids* **28**, 113–128.

Ashby, M. F. 1969. On the Orowan stress. In: *Physics of Strength and Plasticity* (edited by Argon, A. S.). M.I.T. Press, Cambridge, Mass., 113–131.

Bayly, M. B. 1969. Anisotropy of viscosity in suspensions of parallel flakes. *J. Compos. Mater.* **3**, 705–708.

Bayly, M. B. & Cobbold, P. R. 1979. Simple derivation of a shortening/rotation relation for straight lines on symmetrical folds. *Tectonophysics* **53**, T1–T5.

Borradaile, G. H. 1981. Particulate flow of rock and the formation of cleavage. *Tectonophysics* **72**, 305–321.

Cobbold, P. R., Cosgrove, J. W. & Summers, J. M. 1971. Development of internal structures in deformed anisotropic rocks. *Tectonophysics* **12**, 23–53.

Cosgrove, J. W. 1976. The formation of crenulation cleavage. *J. geol. Soc. Lond.* **132**, 155–178.

Dillamore, I. L., Roberts, J. G. & Bush, A. C. 1979. Occurrence of shear bands in heavily rolled cubic metals. *Met. Sci. J.* **13**, 73–77.

Etchecopar, A. 1977. A plane kinematic model of progressive deformation in a polycrystalline aggregate. *Tectonophysics* **39**, 121–139.

Etheridge, M. A., Hobbs, B. E. & Paterson, M. S. 1973. Experimental deformation of single crystals of biotite. *Contr. Miner. Petrol.* **38**, 21–36.

Fletcher, R. C. 1977. Quantitative theory for metamorphic differentiation in development of crenulation cleavage. *Geology* **5**, 185–187.

Granath, J. W. 1980. Strain, metamorphism, and the development of differentiated crenulation cleavages at Cooma, Australia. *J. Geol.* **88**, 589–601.

Gray, D. R. 1979. Microstructure of crenulation cleavages: an indicator of cleavage origin. *Am. J. Sci.* **279**, 97–128.

Glen, J. W. 1974. The physics of ice. U.S. Cold Regions Research and Engineering Laboratory. *Cold Regions Science and Engineering*. Hanover, N.H., Pt II, Sect. C2a, 1–77.

Hirth, J. P. & Lothe, J. 1968. *Theory of Dislocations*. McGraw-Hill, New York.

Kamb, W. B. 1961. The glide direction in ice. *J. Glaciol.* **3**, 1097–1106.

Knipe, R. J. 1981. The interaction of deformation and metamorphism in slates. *Tectonophysics* **78**, 249–272.

Latham, J. P. 1979. Experimentally developed folds in a material with a planar mineral fabric. *Tectonophysics* **57**, T1–T8.

Means, W. D. 1977. Experimental contributions to the study of foliations in rocks: a review of research since 1960. *Tectonophysics* **39**, 329–354.

Means, W. D. 1981. The concept of steady-state foliation. *Tectonophysics* **78**, 179–199.

Means, W. D. & Williams, P. F. 1972. Crenulation cleavage and faulting in an artificial salt–mica schist. *J. Geol.* **80**, 569–591.

Means, W. D., Williams, P. F. & Hobbs, B. E. in press. Incremental deformation and fabric development in a KCl/mica mixture. *J. Struct. Geol.*

Oertel, G. & Phakey, P. P. 1972. The texture of a slate from Nantle, Caenarvon, North Wales. *Texture* **1**, 1–8.

Paterson, M. S. & Weiss, L. E. 1966. Experimental deformation and folding of phyllite. *Bull. geol. Soc. Am.* **77**, 343–374.

Reches, Z. & Johnson, A. M. 1976. A theory of concentric, kink and sinusoidal folding and of monoclinal flexuring of compressible elastic multilayers—VI. Asymmetric folding and monoclinal kinking. *Tectonophysics* **35**, 295–334.

Schmidt, W. 1932. *Tektonik und Verformungslehre*. Borntraeger, Berlin.

Shelley, D. 1974. Mechanical production of metamorphic banding—a critical appraisal. *Geol. Mag.* **111**, 287–292.

Tullis, T. E. 1976. Experiments on the origin of slaty cleavage and schistosity. *Bull. geol. Soc. Am.* **87**, 745–753.

Vidale, R. 1974. Metamorphic differentiation layering in pelitic rocks of Dutchess County, New York. In: *Geochemical Transport and Kinetics* (edited by Hofmann, A. W., Giletti, B. J., Hinthorne, J. B., Andersen, C. A. & Comaford, D.) Carnegie Inst. Wash. Publ. **634**, 273–286.

Weber, K. 1981. Kinematic and metamorphic aspects of cleavage formation in very low-grade metamorphic slates. *Tectonophysics* **78**, 291–306.

Weertman, J. 1968. Diffusion law for the dispersion of hard particles in an ice matrix that undergoes simple shear deformation. *J. Glaciol.* **7**, 161–165.

Weiss, L. E. 1980. Nucleation and growth of kink bands. *Tectonophysics* **65**, 1–38.

Williams, P. F. 1972. Development of metamorphic layering and cleavage in low-grade metamorphic rocks at Bermagui, Australia. *Am. J. Sci.* **272**, 1–47.

Wilson, C. J. L. 1980. Shear zones in a pegmatite: a study of albite–mica–quartz deformation. *J. Struct. Geol.* **2**, 203–209.

Wilson, C. J. L. 1983. Foliation and strain development in ice–mica models. *Tectonophysics* **92**, 93–122.

Wilson, C. J. L. & Russell-Head, D. S. 1982. Steady state preferred orientation of ice deformed in plane strain at −1°C. *J. Glaciol.* **28**, 145–160.